Heterogeneity in old fibroblasts is linked to variability in reprogramming and wound healing

https://doi.org/10.1038/s41586-019-1658-5

Received: 31 March 2016

Accepted: 5 September 2019

Published online: 23 October 2019

Salah Mahmoudi[1,11], Elena Mancini[1,11], Lucy Xu[1,2], Alessandra Moore[3,4], Fereshteh Jahanbani[1], Katja Hebestreit[1], Rajini Srinivasan[4,5], Xiyan Li[1], Keerthana Devarajan[1], Laurie Prélot[1], Cheen Euong Ang[4,6,7], Yohei Shibuya[4,7], Bérénice A. Benayoun[1,10], Anne Lynn S. Chang[8], Marius Wernig[4,7], Joanna Wysocka[4,5], Michael T. Longaker[3,4], Michael P. Snyder[1] & Anne Brunet[1,9]*

Age-associated chronic inflammation (inflammageing) is a central hallmark of ageing[1], but its influence on specific cells remains largely unknown. Fibroblasts are present in most tissues and contribute to wound healing[2,3]. They are also the most widely used cell type for reprogramming to induced pluripotent stem (iPS) cells, a process that has implications for regenerative medicine and rejuvenation strategies[4]. Here we show that fibroblast cultures from old mice secrete inflammatory cytokines and exhibit increased variability in the efficiency of iPS cell reprogramming between mice. Variability between individuals is emerging as a feature of old age[5–8], but the underlying mechanisms remain unknown. To identify drivers of this variability, we performed multi-omics profiling of fibroblast cultures from young and old mice that have different reprogramming efficiencies. This approach revealed that fibroblast cultures from old mice contain 'activated fibroblasts' that secrete inflammatory cytokines, and that the proportion of activated fibroblasts in a culture correlates with the reprogramming efficiency of that culture. Experiments in which conditioned medium was swapped between cultures showed that extrinsic factors secreted by activated fibroblasts underlie part of the variability between mice in reprogramming efficiency, and we have identified inflammatory cytokines, including TNF, as key contributors. Notably, old mice also exhibited variability in wound healing rate in vivo. Single-cell RNA-sequencing analysis identified distinct subpopulations of fibroblasts with different cytokine expression and signalling in the wounds of old mice with slow versus fast healing rates. Hence, a shift in fibroblast composition, and the ratio of inflammatory cytokines that they secrete, may drive the variability between mice in reprogramming in vitro and influence wound healing rate in vivo. This variability may reflect distinct stochastic ageing trajectories between individuals, and could help in developing personalized strategies to improve iPS cell generation and wound healing in elderly individuals.

Several studies have investigated the effect of ageing and senescence on reprogramming[9–12], but a systematic evaluation of how ageing influences reprogramming is lacking. We examined the influence of old age on the inflammatory profile of fibroblasts and their ability to reprogram to iPS cells (Fig. 1a). Using cytokine profiling, we compared the systemic milieu (plasma) and conditioned medium from primary fibroblast cultures from young (3 months) and old (28–29 months) mice (Fig. 1a). Plasma from old mice showed increased levels of pro-inflammatory cytokines (for example, IL-6 and TNF), anti-inflammatory cytokines (for example, IL-4), and chemokines and growth factors (for example, CSF1 (also known as MCSF)) compared to plasma from young mice (Fig. 1b, Extended Data Fig. 1a, b and Supplementary Table 1a). Conditioned medium from primary fibroblast cultures from the ears of old mice also showed enhanced levels of pro- and anti-inflammatory cytokines (for example, IL-6 and TNF, and IL-4, respectively; (Fig. 1b, Extended Data Fig. 1c, d and Supplementary Table 1b). Similarly, inflammatory cytokines increased with

[1]Department of Genetics, Stanford University, Stanford, CA, USA. [2]Department of Biology, Stanford University, Stanford, CA, USA. [3]Department of Surgery, Division of Plastic and Reconstructive Surgery, Stanford University, Stanford, CA, USA. [4]Institute for Stem Cell Biology and Regenerative Medicine, Stanford University, Stanford, CA, USA. [5]Department of Chemical and Systems Biology, Stanford University, Stanford, CA, USA. [6]Department of Bioengineering, Stanford University, Stanford, CA, USA. [7]Department of Pathology, Stanford University, Stanford, CA, USA. [8]Department of Dermatology, Stanford University, Stanford, CA, USA. [9]Glenn Laboratories for the Biology of Aging, Stanford University, Stanford, CA, USA. [10]Present address: Leonard Davis School of Gerontology, University of Southern California, Los Angeles, CA, USA. [11]These authors contributed equally: Salah Mahmoudi, Elena Mancini. *e-mail: anne.brunet@stanford.edu

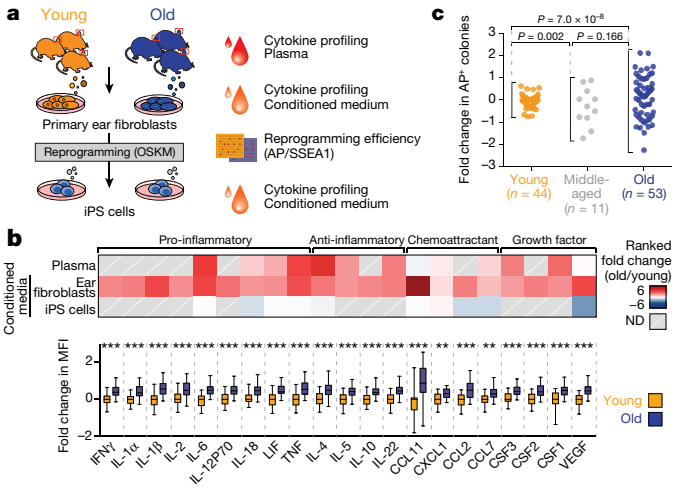

Fig. 1 | Primary fibroblasts from old mice secrete inflammatory cytokines and show increased variability in reprogramming efficiency between mice. **a**, Experimental schematic. Young mice, 3 months old; old mice, 28–29 months old. OSKM, *OCT4*, *SOX2*, *KLF4* and *MYC*. **b**, Top, age-dependent changes in cytokine levels in plasma and conditioned medium from fibroblasts or iPS cells (Extended Data Fig. 1a, g, h). ND, not detected. Bottom, cytokine profiles of conditioned medium from primary cultures (passage 3) of ear fibroblasts from young (3 months, $n = 24$) and old (29 months, $n = 24$) male mice (3 independent experiments). Box-and-whisker plots of $\log_2$-transformed fold change in mean fluorescence intensity (MFI) compared to the median of young fibroblasts. Box plots depict median and interquartile range, with whiskers indicating minimum and maximum values. $^{**}P < 0.01$, $^{***}P < 0.001$; two-tailed Wilcoxon rank-sum test with Benjamini–Hochberg correction. Exact P values can be found in Supplementary Table 1b. **c**, Reprogramming efficiency assessed by alkaline phosphatase (AP) staining of cultures of ear fibroblasts obtained from young (3 months, $n = 44$), middle-aged (12 months, $n = 11$) and old (28–29 months, $n = 53$) mice (7 independent experiments). The $\log_2$-transformed fold change over the median of young mice is shown. Each dot represents a fibroblast culture from one mouse. P values, Fligner–Killeen test to assess differences in variance between age groups with Benjamini–Hochberg correction.

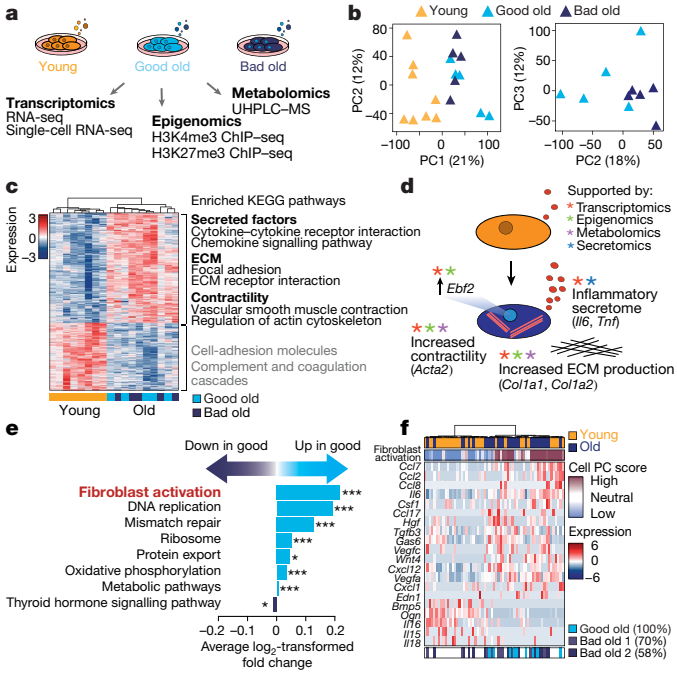

Fig. 2 | Old fibroblast cultures exhibit a signature of an inflammatory activated state, which is associated with variability in reprogramming efficiency. **a**, Multi-omics characterization of fibroblast cultures. ChIP–seq, chromatin immunoprecipitation followed by sequencing; UHPLC–MS, ultra-high performance liquid chromatography–tandem mass spectrometry. **b**, Principal component (PC) analysis of transcriptomes cultures of ear fibroblasts from young (3 months, $n = 8$) and old (29 months, $n = 10$) (left) or only old (right) mice (3 independent experiments). Old cultures were either good (high reprogramming efficiency) or bad (low reprogramming efficiency) (Supplementary Table 2a). **c**, Heat map of significantly differentially expressed genes (determined by DESeq2) between young and old fibroblasts described in **b** and enriched Kyoto Encyclopedia of Genes and Genomes (KEGG) pathways. Pathways are colour coded according to significance (one-sided Fisher's exact test with Benjamini–Hochberg correction; black, false-discovery rate (FDR)-adjusted $P < 0.05$; grey, FDR-adjusted $P < 0.15$; Supplementary Table 2b, c). ECM, extracellular matrix. **d**, Summary of the multi-omics profiling of young and old fibroblast cultures (Extended Data Fig. 2). **e**, Pathway enrichment analysis of KEGG pathways associated with good or bad reprogramming efficiency. Overlapping significant (FDR-adjusted $P < 0.05$) KEGG pathways identified in a regression analysis from bad to good reprogramming efficiencies ($n = 18$) and in a separate analysis comparing the five highest and five lowest reprogramming efficiency cultures (exact P values can be found in Supplementary Table 3b, d). $^{*}P < 0.05$, $^{***}P < 0.001$; two-sided nominal P value with Benjamini–Hochberg correction. **f**, PAGODA of single-cell RNA-seq from young ($n = 30$ cells), good and bad old ($n = 31$ cells) fibroblasts. Top heat maps, PAGODA clustering of cells. For cell PC score, maroon and blue colours indicate increased and decreased expression of the associated gene sets, respectively. Middle heat map, expression of specific cytokine genes (Extended Data Fig. 4g). Bottom heat map, single cells from good and bad old fibroblast cultures. Gene expression is shown as VST-transformed (variance stabilizing transformation, implemented in DESeq2) read counts scaled row-wise.

age in conditioned medium from lung fibroblasts and human primary fibroblasts (Extended Data Fig. 1e, f and Supplementary Table 1c, d). Thus, primary cultures of fibroblasts from old mice exhibit a secretory inflammatory profile that overlaps in part with that of the systemic milieu (Fig. 1b and Extended Data Fig. 1h).

To systematically test the effect of age on iPS cell reprogramming, we derived independent fibroblast cultures from a total of 108 young, middle-aged and old mice. We induced reprogramming by expressing human *OCT4* (also known as *POU5F1*), *KLF4*, *SOX2* and *MYC*[13], and assessed reprogramming efficiency using alkaline phosphatase (AP) and stage-specific embryonic antigen 1 (SSEA1) staining[10] (Fig. 1a and Extended Data Fig. 1i–l). We did not observe a significant change in mean reprogramming efficiency with age (Fig. 1c and Extended Data Fig. 1l). However, there was increased variability between mice in reprogramming efficiency with age, with cultures from some old mice reprogramming better and some worse than cultures from young mice (Fig. 1c and Extended Data Fig. 1l). A similar age-dependent increase in variability in reprogramming efficiency was observed in chest fibroblast cultures (Extended Data Fig. 1m). Reprogramming efficiency appeared to be inherent to each culture (derived from an individual mouse), as the same culture exhibited largely consistent reprogramming efficiency to iPS cells between independent experiments or to induced neurons (Extended Data Fig. 1n, o). This increased variability in reprogramming efficiency between fibroblast cultures from different old mice could reflect distinct stochastic ageing trajectories.

Variability between old individuals has been observed for several biological features[5–8]. However, most studies were performed in humans, in which genetic and environmental differences also have a role. We used the controlled mouse system to understand the stochastic variability in reprogramming efficiency between cultures from old mice. Using a multi-omics approach, we profiled the transcriptomes, epigenomes and metabolomes of young fibroblasts as well as old fibroblasts that reprogrammed well (good old) or poorly (bad old) (Fig. 2a and Supplementary Table 2a). Principal component analysis and unsupervised hierarchical clustering showed a separation between young and old fibroblasts across datasets (Fig. 2b and Extended Data Fig. 2a–h). Principal component analysis also revealed some separation between the

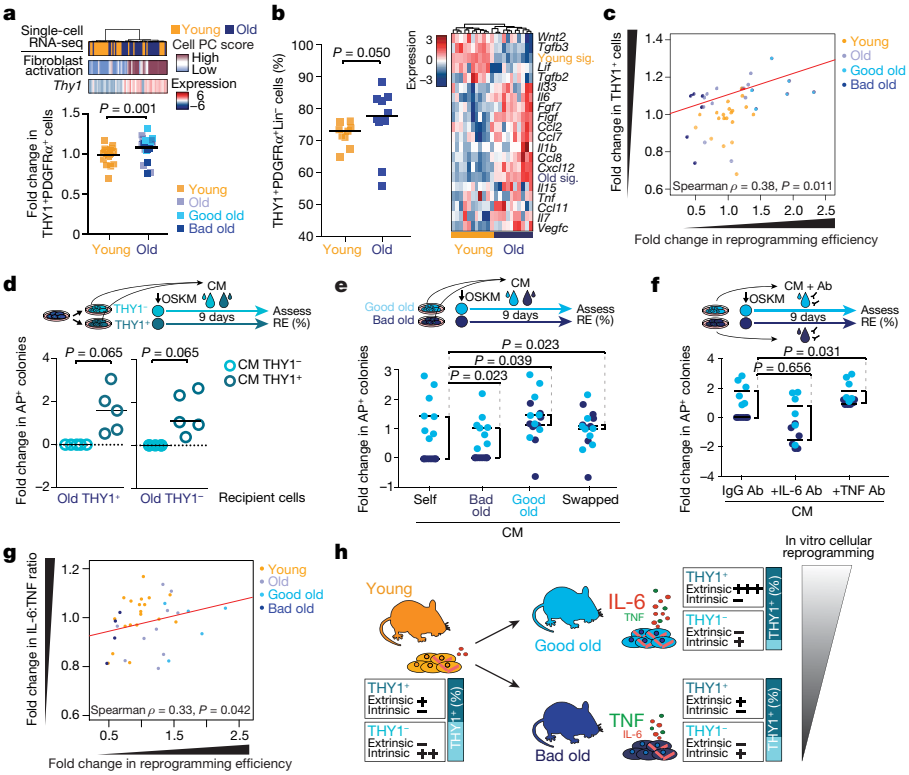

Fig. 3 | Age-associated increase in activated fibroblasts and the cytokines that they secrete drive part of the variability in reprogramming between mice. a, Top, PAGODA clustering of single-cell RNA-seq data from young and old fibroblasts as in Fig. 2f, showing *Thy1* expression. Bottom, proportion of THY1$^+$PDGFRα$^+$ fibroblasts in fibroblast cultures of young (3 months, $n = 21$) and old (29 months, $n = 23$) mice measured by FACS (3 independent experiments). Fold changes were calculated relative to the median of young mice. *P* value, two-tailed Wilcoxon rank-sum test. Each dot represents a culture from one mouse. Lines depict median. **b**, Left, Percentage of THY1$^+$PDGFRα$^+$Lin$^-$ out of all PDGFRα$^+$Lin$^-$ fibroblasts isolated from ears of young mice (3–4 months, $n = 9$ replicates, each with 2–3 mice) and old mice (24–26 months, $n = 10$ replicates, each with 2–3 mice) analysed by FACS (3 independent experiments). *P* value as in **a**. Each dot represents a replicate, with cells pooled from 2–3 mice. Lines depict median. Right, heat map of the expression of specific cytokine genes from population RNA-seq of fibroblasts. VST-transformed read counts are shown scaled row-wise. Young sig. and old sig. indicate the average expression of genes that are significantly downregulated and upregulated with age, respectively. **c**, Spearman's correlation between the proportion of THY1$^+$PDGFRα$^+$ (THY1$^+$) fibroblasts in a given culture (quantified by FACS) and the reprogramming efficiency (assessed as in Fig. 1c) of that culture (ages as in **a**; young, $n = 21$; old, $n = 23$; 3 independent experiments). Fold changes relative to the median of young mice. *P* values, two-sided algorithm AS 89 in R. Each dot represents a culture from one mouse. **d**, Reprogramming efficiency (RE) of FACS-sorted old THY1$^+$PDGFRα$^+$ (THY1$^+$) and THY1$^-$PDGFRα$^+$ (THY1$^-$) fibroblasts treated daily with conditioned medium (CM) from THY1$^-$PDGFRα$^+$ or THY1$^+$PDGFRα$^+$ fibroblasts from the same original culture. $\log_2$-transformed fold change relative to THY1$^-$PDGFRα$^+$ fibroblasts treated with conditioned medium from THY1$^-$PDGFRα$^+$ fibroblasts ($n = 5$ old mice, 4 independent experiments). *P* values, two-tailed Wilcoxon signed-rank test. Each dot represents a culture from one mouse. Lines depict median. **e**, Reprogramming efficiency of pairs of good old and bad old fibroblast cultures treated with their own conditioned medium (self conditioned medium) or conditioned medium from the other group (swapped conditioned medium). $\log_2$-transformed fold change relative to bad old self conditioned medium. $n = 8$ pairs of good and old bad cultures (5 independent experiments). *P* values, two-tailed Wilcoxon signed-rank test with Benjamini–Hochberg correction. Each dot represents a culture from one mouse. Lines depict median. **f**, Reprogramming efficiency of pairs of good old and bad old fibroblast cultures treated with their own conditioned medium, which was pretreated with blocking antibodies. $\log_2$-transformed fold change in reprogramming efficiency relative to bad old conditioned medium treated with IgG antibodies. $n = 6$ pairs of good old and bad old cultures (4 independent experiments). *P* values, two-tailed Wilcoxon signed-rank test with Benjamini–Hochberg correction. Each dot represents a culture from one mouse. Lines depict median. **g**, Spearman's correlation between conditioned medium and the ratio of IL-6 and TNF levels in the conditioned medium (young, $n = 19$; old, $n = 18$; ages as in **a**; 2 independent experiments). Fold change relative to the median of young mice. *P* values, two-sided algorithm AS 89 in R. Each dot represents a culture from one mouse. **h**, Model for the increased variability in cellular reprogramming between mice in vitro.

transcriptomes and metabolomes of good old and bad old cultures (Fig. 2b and Extended Data Fig. 2i, j).

Old fibroblasts showed transcriptional enrichment of pathways related to secreted factors (for example, cytokine signalling), extracellular matrix, contractility, inflammation and wound healing (Fig. 2c, d, Extended Data Fig. 2k, l and Supplementary Table 2b–e). These features are characteristic of activated fibroblasts (also known as myofibroblasts), which are normally involved in tissue repair[2,3,14,15]. Indeed, the 'fibroblast activation' gene set was enriched in the old fibroblast transcriptomes (Extended Data Fig. 2m and Supplementary Table 2f). Epigenomic and metabolomics changes supported this fibroblast activation signature (Fig. 2d, Extended Data Fig. 2n–t and Supplementary Table 2g–m). The transcription factor EBF2, which shows increased expression in old fibroblasts, was identified as a potential driver of this activated fibroblast signature (Fig. 2d, Extended Data Fig. 2q, u and Supplementary Table 2n). Primary fibroblast cultures from elderly humans also exhibited increased *EBF2* and cytokine-related pathway expression (Extended Data Fig. 2v, Supplementary Table 2o, p). Notably, fibroblast activation was a top feature associated with good reprogramming of old fibroblasts in both transcriptomic and epigenomic datasets (Fig. 2e, Extended Data Fig. 2w and Supplementary Table 3a–f). Hence, the fibroblast activation signature is enriched in old fibroblasts and correlates with the variability between mice in reprogramming.

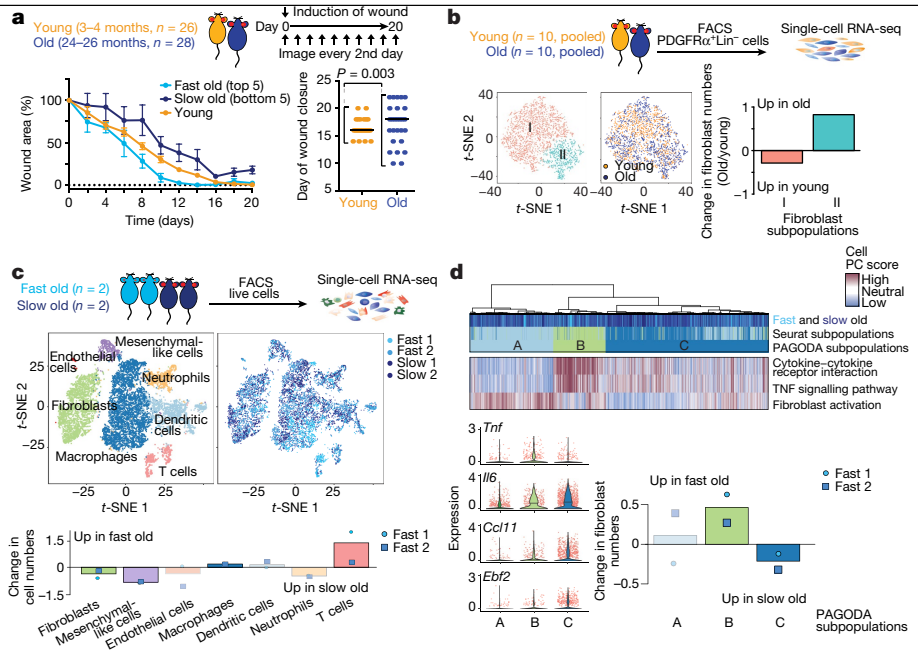

Fig. 4 | Wound healing rate is variable between old mice and correlates with fibroblast subpopulations with distinct cytokine signatures. a, Ear wound healing assays in young (3–4 months, $n = 26$) and old (24–26 months, $n = 28$) mice (2 independent experiments). Left, ear wound healing curves from young mice and the five fastest- and five slowest-healing old mice. Percentage of wound area that remains on the indicated day (mean ± s.d.) Right, day of ear wound closure in young and old mice. Each dot represents one mouse. Line marks median. *P* values, Fligner–Killeen test to assess difference in variance between age groups. **b**, Single-cell RNA-seq of FACS-sorted PDGFRα$^+$Lin$^-$ cells from the ear wounds of young mice (3–4 months, cells pooled from $n = 10$ mice) or old mice (24–26 months, cells pooled from $n = 10$ mice), 7 days after induction of wounds. Left, *t*-distributed stochastic neighbour embedding (*t*-SNE) clustering of cells (3,036 total; 1,592 young, 1,444 old) coloured by Seurat clusters or age. Right, $\log_2$-transformed fold change in the subpopulations between wounds of young and old mice. **c**, Single-cell RNA-seq of live cells from entire wounds of old mice (24 months) with fast-healing ($n = 2$) and slow-healing ($n = 2$) trajectories, 7 days after induction of wounds. *t*-SNE clustering of cells ($n = 10{,}797$ total), coloured by Seurat clusters or mouse (slow old 1, $n = 3{,}761$; slow old 2, $n = 2{,}127$; fast old 1, $n = 2{,}533$; fast old 2, $n = 2{,}376$). Bottom, $\log_2$-transformed fold change in the cell types between wounds from fast-healing compared to slow-healing old mice. **d**, PAGODA clustering of cells ($n = 2{,}678$ total; slow old 1, $n = 1{,}087$; slow old 2, $n = 551$; fast old 1, $n = 441$; fast old 2, $n = 599$) identified as fibroblasts in **c**. Top heat map, single cells from wounds from old mice with fast- and slow-healing trajectories. Bottom heat map, separation of cells based on principal component scores for a subset of the top significantly overdispersed gene sets. For cell PC score, maroon and blue colours indicate generally increased and decreased expression of the associated gene sets, respectively. $\log_2$-transformed and normalized gene expression values calculated by Seurat and scaled row-wise. Bottom left, $\log_2$-normalized expression values of relevant genes. Each dot represents a single cell. Line marks median. Bottom right, $\log_2$-tranformed fold change in the number of cells in each of the three fibroblast subpopulations identified by PAGODA.

We wondered whether age-dependent cellular heterogeneity[8,16–19] could contribute to the variability between individual mice. To determine whether fibroblast cultures are heterogeneous, we performed single-cell RNA sequencing (RNA-seq) on young, good old and bad old cultures. Although the number of single cells profiled was low, the good old culture contained a higher proportion of activated cells compared to the two bad old cultures (Fig. 2f, Extended Data Fig. 4a–g and Supplementary Table 3g). Thus, the proportion of activated fibroblasts may be linked to the variability in reprogramming between individual cultures.

We validated that old fibroblast cultures were enriched in activated cells by staining for α-smooth muscle actin (αSMA), a marker of activated fibroblasts[2,3,14,15] (Extended Data Fig. 5a). These activated fibroblasts were proliferating and did not exhibit senescence markers (for example, *p16*^{Ink4a}) (Extended Data Fig. 5b–e). Fluorescence-activated cell sorting (FACS) analysis of the pan-fibroblast marker PDGFRα[3,14,19] as well as THY1[20], which correlates with the activated fibroblast signature, confirmed that old fibroblast cultures contained higher proportions of THY1$^+$PDGFRα$^+$ cells (Fig. 3a and Supplementary Table 4a–c). THY1$^+$PDGFRα$^+$ cells expressed fibroblast activation markers, inflammatory cytokines and *Ebf2* (Extended Data Fig. 5f). *Ebf2* knockdown in these cells reduced expression of fibroblast activation genes (for example, *Acta2* (which encodes αSMA), *Il6* and *Ccl11* (also known as *Eotaxin*)), whereas *Ebf2* overexpression in young fibroblasts induced expression of cytokines (for example, *Il6*; Extended Data Fig. 5g, h). In vivo FACS analysis also revealed a higher proportion of THY1$^+$PDGFRα$^+$ fibroblasts in the ears of old mice (Fig. 3b), and these fibroblasts exhibited a fibroblast activation signature with expression of inflammatory cytokines (Fig. 3b, Extended Data Fig. 5i–k and Supplementary Table 4d–g). Thus, activated fibroblasts are enriched in old cultures and old tissues in vivo.

Notably, FACS analysis of fibroblast cultures corroborated the positive correlation between the proportion of activated (THY1$^+$PDGFRα$^+$) fibroblasts in a culture and the ability of this culture to reprogram (Fig. 3c and Extended Data Fig. 5l–n). Reprogramming efficiency also correlated positively with proliferation and negatively with senescence (Extended Data Fig. 5o, p). Thus, the proportion of activated fibroblasts, though not more variable with age, correlates positively with reprogramming efficiency.

We next investigated how activated fibroblasts influence reprogramming efficiency. Activated THY1$^+$PDGFRα$^+$ fibroblasts intrinsically reprogrammed less efficiently than their non-activated THY1$^-$PDGFRα$^+$ counterparts (Extended Data Fig. 5q, r). By contrast, conditioned medium from activated fibroblasts enhanced reprogramming (of both activated and non-activated fibroblasts) compared to medium from non-activated fibroblasts (Fig. 3d, Extended Data Fig. 5s–u and Supplementary Table 4h). Therefore, activated fibroblasts have opposing intrinsic and extrinsic effects on reprogramming efficiency, and the relative proportions of activated and non-activated fibroblasts in cultures from old mice could underlie the variability in reprogramming efficiency.

To analyse whether extrinsic factors drive the variability in reprogramming efficiency between individual old cultures, we examined the difference in reprogramming efficiency between good and bad old fibroblast cultures, treated with their own conditioned medium or conditioned medium that was swapped between cultures (Fig. 3e and Extended Data Fig. 6a–c). Reprogramming pairs of good and bad old cultures with swapped conditioned medium reduced the difference between their reprogramming efficiencies (Fig. 3e) by more than 60% (Extended Data Fig. 6c). Extrinsic factors thus have a substantial role in the variability in reprogramming efficiency between old cultures, and intrinsic factors are likely to underlie the remainder of the effect.

We next tested whether cytokines contribute to the role of extrinsic factors on the variability between mice. IL-6, TNF and IL-1β, which are all secreted by old fibroblast cultures, affected reprogramming in opposing directions: IL-6 enhanced reprogramming efficiency (as previously reported[21]), whereas TNF and IL-1β impaired reprogramming efficiency in young and old fibroblasts (Extended Data Fig. 6d–i). Consistently, blocking IL-6 with an antibody reduced reprogramming efficiency, whereas blocking TNF improved it (Extended Data Fig. 6j, k). To determine whether IL-6 and TNF contributed to the variability between mice in reprogramming efficiency, we reprogrammed pairs of good old and bad old fibroblast cultures in their own conditioned medium, which was pretreated with IL-6- or TNF-blocking antibodies. While blocking IL-6 had a minor effect, blocking TNF reduced the difference in reprogramming efficiency between pairs of good old and bad old cultures (Fig. 3f) by more than 40% (Extended Data Fig. 6l–n). The IL-6:TNF ratio correlated with reprogramming efficiency (Fig. 3g and Extended Data Fig. 6o–q). Hence, the proportions of activated and non-activated fibroblasts, and the ratio of inflammatory cytokines that they secrete (for example, IL-6 and TNF), could drive the variability between fibroblast cultures of different old mice (Fig. 3h).

Fibroblasts are critical for wound healing in vivo[2,3,14,15]. Although the influence of ageing on wound healing has been examined[2,15,22,23], the variability of this response is not known. We assessed the rate of healing in wounds on the ears of young and old mice (Fig. 4a). While the median wound healing rate was not significantly affected by age, there was an increased variability in wound healing rate between old mice, with some old mice healing faster and some slower than young mice (Fig. 4a and Extended Data Fig. 7a–g).

To determine the overall fibroblast composition in wounds from young and old mice, we performed single-cell RNA-seq on FACS-sorted fibroblasts pooled from the wounds of 10 young or 10 old mice, 7 days after the induction of wounds—irrespective of wound healing rates (Fig. 4b and Extended Data Fig. 7c, d). Fibroblast composition changed in wounds from old mice in vivo (Fig. 4b), with subpopulations of fibroblasts exhibiting signatures of fibroblast activation and increased cytokine signalling (Extended Data Fig. 8a–f).

We next performed single-cell RNA-seq on all cells from the wounds of old mice with slow- or fast-healing trajectories (Fig. 4c and Extended Data Fig. 8g–i). Although epithelial cells were not identified (perhaps owing to the isolation protocol or wound composition and as previously reported[14]), fibroblasts, endothelial cells and immune cells were identified (Fig. 4c and Extended Data Fig. 8j). Notably, fibroblasts were more abundant in wounds of slow-healing old mice, whereas immune cells were more abundant in wounds of fast-healing old mice (Fig. 4c and Supplementary Table 5e). Although the number of mice is low and differences in the composition of cells could also be influenced by wound stage and isolation properties, fibroblast populations may therefore be associated with distinct wound healing trajectories.

Clustering using both Seurat and pathway and gene set overdispersion analysis (PAGODA) on wound fibroblasts from slow-healing or fast-healing old mice identified three main subpopulations (A, B and C) that were enriched in different aspects of fibroblast activation (Fig. 4d and Extended Data Fig. 9d, e; for a combined analysis of both single-cell RNA-seq datasets, see Extended Data Fig. 9h–l). Whereas fibroblast subpopulation A was present in wounds of both slow- and fast-healing mice, fibroblast subpopulation B was more abundant in wounds of fast-healing old mice and exhibited increased cytokine expression and signalling (for example, *Tnf*; Fig. 4d, Extended Data Fig. 9d, f, k and Supplementary Table 5f, g). Thus, TNF is associated with fast wound healing in vivo and bad reprogramming in vitro (fast wound healing might lead to fibrosis, which is detrimental). By contrast, fibroblast subpopulation C was more abundant in wounds from slow-healing old mice and exhibited higher expression of other cytokines (for example, *Ccl11*) and the transcription factor *Ebf2* (Fig. 4d, Extended Data Fig. 9d–g, k and Supplementary Table 5f, g). Activated fibroblast subpopulations with distinct cytokine profiles (for example, TNF compared to IL-6 or CCL11) may therefore be associated with increased variability in reprogramming in vitro and wound healing trajectories in old mice.

Our study shows that ageing is associated with an increased variability between mice in cellular reprogramming in vitro and in wound healing in vivo, perhaps reflecting different ageing trajectories. Increased variability is emerging as common feature of ageing[5–8], and we identify inflammatory cytokines, including TNF, as key contributing factors to variability in reprogramming efficiency (although other intrinsic and extrinsic factors may also exist). Cytokine signalling may also regulate the variability in other ageing phenotypes, including wound healing. Dermal fibroblasts have been shown to lose cellular identity and acquire adipogenic traits during ageing[19], and this increased cellular heterogeneity could also contribute to the differences between individual mice. As fibroblasts exhibit tissue-specific properties, variability in distinct tissues may differentially increase with age.

A subpopulation of activated fibroblasts could be a source of chronic inflammation in old individuals and contribute to immune cell recruitment[3,14,15,20]. Activated fibroblasts (which proliferate) and senescent fibroblasts (which show permanent cell cycle arrest) secrete overlapping yet distinct sets of cytokines[24] and may interact in a complex manner to influence reprogramming and wound healing. Wound healing is a major issue for elderly individuals, with either deficient wound healing (which can lead to ulcers) or excessive wound healing (which can lead to fibrosis)[2,3,15]. Changes in fibroblast subpopulations and cytokines with age could contribute to these pathologies and constitute targets for personalized strategies to restore functional wound healing in elderly individuals.

Online content

Any methods, additional references, Nature Research reporting summaries, source data, extended data, supplementary information, acknowledgements, peer review information; details of author contributions and competing interests; and statements of data and code availability are available at https://doi.org/10.1038/s41586-019-1658-5.

1. Franceschi, C. & Campisi, J. Chronic inflammation (inflammaging) and its potential contribution to age-associated diseases. *J. Gerontol. A Biol. Sci. Med. Sci.* **69**, S4–S9 (2014).
2. Eming, S. A., Martin, P. & Tomic-Canic, M. Wound repair and regeneration: mechanisms, signaling, and translation. *Sci. Transl. Med.* **6**, 265sr6 (2014).
3. Lynch, M. D. & Watt, F. M. Fibroblast heterogeneity: implications for human disease. *J. Clin. Invest.* **128**, 26–35 (2018).
4. Ocampo, A., Reddy, P. & Belmonte, J. C. I. Anti-aging strategies based on cellular reprogramming. *Trends Mol. Med.* **22**, 725–738 (2016).
5. Chaleckis, R., Murakami, I., Takada, J., Kondoh, H. & Yanagida, M. Individual variability in human blood metabolites identifies age-related differences. *Proc. Natl Acad. Sci. USA* **113**, 4252–4259 (2016).
6. Ong, M. L. & Holbrook, J. D. Novel region discovery method for Infinium 450K DNA methylation data reveals changes associated with aging in muscle and neuronal pathways. *Aging Cell* **13**, 142–155 (2014).
7. Li, R. et al. Linking inter-individual variability in functional brain connectivity to cognitive ability in elderly individuals. *Front. Aging Neurosci.* **9**, 385 (2017).
8. Cheung, P. et al. Single-cell chromatin modification profiling reveals increased epigenetic variations with aging. *Cell* **173**, 1385–1397 (2018).
9. Lapasset, L. et al. Rejuvenating senescent and centenarian human cells by reprogramming through the pluripotent state. *Genes Dev.* **25**, 2248–2253 (2011).

10. Li, H. et al. The *Ink4/Arf* locus is a barrier for iPS cell reprogramming. *Nature* **460**, 1136–1139 (2009).
11. Ravaioli, F., Bacalini, M. G., Franceschi, C. & Garagnani, P. Age-related epigenetic derangement upon reprogramming and differentiation of cells from the elderly. *Genes* **9**, 39 (2018).
12. Mosteiro, L. et al. Tissue damage and senescence provide critical signals for cellular reprogramming in vivo. *Science* **354**, aaf4445 (2016).
13. Somers, A. et al. Generation of transgene-free lung disease-specific human induced pluripotent stem cells using a single excisable lentiviral stem cell cassette. *Stem Cells* **28**, 1728–1740 (2010).
14. Guerrero-Juarez, C. F. et al. Single-cell analysis reveals fibroblast heterogeneity and myeloid-derived adipocyte progenitors in murine skin wounds. *Nat. Commun.* **10**, 650 (2019).
15. Shook, B. A. et al. Myofibroblast proliferation and heterogeneity are supported by macrophages during skin repair. *Science* **362**, eaar2971 (2018).
16. Frenk, S. & Houseley, J. Gene expression hallmarks of cellular ageing. *Biogerontology* **19**, 547–566 (2018).
17. Bahar, R. et al. Increased cell-to-cell variation in gene expression in ageing mouse heart. *Nature* **441**, 1011–1014 (2006).
18. Wiley, C. D. et al. Analysis of individual cells identifies cell-to-cell variability following induction of cellular senescence. *Aging Cell* **16**, 1043–1050 (2017).
19. Salzer, M. C. et al. Identity noise and adipogenic traits characterize dermal fibroblast aging. *Cell* **175**, 1575–1590 (2018).
20. Croft, A. P. et al. Distinct fibroblast subsets drive inflammation and damage in arthritis. *Nature* **570**, 246–251 (2019).
21. Brady, J. J. et al. Early role for IL-6 signalling during generation of induced pluripotent stem cells revealed by heterokaryon RNA-seq. *Nat. Cell Biol.* **15**, 1244–1252 (2013).
22. Keyes, B. E. et al. Impaired epidermal to dendritic T cell signaling slows wound repair in aged skin. *Cell* **167**, 1323–1338 (2016).
23. Nishiguchi, M. A., Spencer, C. A., Leung, D. H. & Leung, T. H. Aging suppresses skin-derived circulating SDF1 to promote full-thickness tissue regeneration. *Cell Rep.* **24**, 3383–3392 (2018).
24. Coppé, J. P. et al. Senescence-associated secretory phenotypes reveal cell-nonautonomous functions of oncogenic RAS and the p53 tumor suppressor. *PLoS Biol.* **6**, e301 (2008).